第34卷 第6期 焊 接 学 报 Vol. 34 No. 6
2013年6月 TRANSACTIONS OF THE CHINA WELDING INSTITUTION June 2013

锰对脉冲燃烧型焊条立焊接头组织性能的影响

吴永胜[1]， 王建江[1]， 辛文彤[1]， 曲立峰[2]
(1. 军械工程学院 先进材料研究所，石家庄 050003；2. 重庆军事代表局驻167厂军事代表室，成都 610110)

摘 要： 用脉冲燃烧型焊条对Q235钢进行了手工自蔓延立焊焊接，研究了焊条锰含量对立焊接头组织性能的影响. 结果表明，脉冲燃烧型焊条中未添加锰时，起焊位置没有形成有效熔池且焊缝中有大量气孔；锰含量低于5.9%(质量分数)时锰含量越高焊缝成形越好，焊缝中气孔迅速减少，焊缝以富铁相为主且富铁相占比随锰含量增加而增加，接头力学性能升高. 锰含量为5.9%(质量分数)时接头力学性能最高，抗拉强度可达421 MPa，显微硬度可达1 578.8 MPa. 锰含量超过5.9%(质量分数)时，锰含量增加使得熔池向下流动严重形成焊瘤，甚至烧穿母材，焊缝以富铜相为主且有大量裂纹出现，力学性能迅速降低.

关键词： 脉冲燃烧型焊条；立焊；组织性能
中图分类号： TG456 **文献标识码：** A **文章编号：** 0253－360X(2013)06－0097－04

吴永胜

0 序 言

手工自蔓延焊接是一种新的自蔓延熔焊方法，该方法以普通燃烧型焊条为焊接材料，通过焊条自身燃烧合成反应产生的热量将焊接母材局部加热熔化，用反应的产物填充焊缝，采用焊条电弧焊的操作方法，实现焊接母材的永久牢固连接[1－3]. 目前手工自蔓延焊接用焊条按焊接位置分两大类，一类是适用平焊为主的普通燃烧型焊条，另一类是适用立焊为主的脉冲燃烧型焊条. 锰作为一般低碳钢和低合金钢焊缝中不可缺少的合金元素，一方面可以与硅一起使焊缝金属充分脱氧；另一方面在钢中具有较强的固溶强化作用，能显著提高焊缝的强度；添加量适当时还能提高焊缝韧性[4]. Mn元素是脉冲燃烧型焊条中一种重要组成元素，添加量达到6%(质量分数). 另一方面却有研究认为焊丝中元素Mn的过渡处于损失状态，并且随着焊丝的Fe_xO_y含量的增加，其损失越来越大[5]. 使用脉冲燃烧型焊条立焊所得接头中的合金元素均由焊条燃烧后熔滴过渡进入焊缝，所以研究焊条中元素Mn的过渡情况和对立焊接头组织性能的影响非常重要.

1 试验方法

脉冲燃烧型焊条由3个高热焊药段和两个低热造渣段交替排列组成[6]. 高热焊药段由高热剂、造渣剂、合金剂和脱氧剂组成，低热造渣段由高热剂、造渣剂和稀释剂组成，把焊药混合均匀后分段装入焊条即可得脉冲燃烧型焊条. 文中试验方案低热造渣段维持不变，高热焊药段配比如表1所示.

表1 试验方案(质量分数，%)
Table 1 Testing scheme

	高热剂	合金剂	造渣剂	锰	其它
1	74.02	15.68	7.04	0	3.26
2	72.50	15.36	6.90	2.04	3.20
3	71.05	15.05	6.76	4.01	3.13
4	69.65	14.75	6.63	5.90	3.07
5	68.31	14.47	6.50	7.72	3.01
6	67.01	14.19	6.38	9.46	2.95

试验所用焊接母材Q235钢板的尺寸为70 mm×40 mm×3 mm，不开坡口，不需要清理母材上的锈蚀. 焊接试验用脉冲燃烧型焊条对Q235钢板不留间隙、无预热对接立焊，焊接时用火柴点燃引火线，引火线段燃烧引燃焊药，焊药发生燃烧合成反应形成燃烧弧，采用焊条电弧焊的运条方法，高热焊药段反应产生的大量热量使母材局部融化，形成熔池，冷却后生成的金属产物填充于焊缝中；低热造渣段热量过低无法形成熔池，生成的熔渣覆盖于金属焊缝之上. 焊后依据国家标准GB/T2649—1989，GB/T2653—1989和GB/T3965—1995中的相关规定，对焊接接头进行了拉伸性能试验，并使用Quanta-FEG

收稿日期：2012－04－17

250 型扫描电镜和 INCA 型能谱仪进行焊接接头的组织分析.

2 试验结果

焊接结束焊件完全冷却后,轻轻敲打清理焊缝表面熔渣,即可获得脉冲燃烧型焊条立焊接头,如图 1 所示. 试验采取向上立焊,下部为起焊位置,由下向上依次为第 1,第 2,第 3 熔池. 1 号试样起焊位置没有形成有效熔池; 2 号试样表面成形良好,但第 1 熔池熔深浅,未焊透; 3 号,4 号试样焊缝成形良好,达到了单面焊双面成形; 5 号试样熔池下流较严重,在下部形成焊瘤; 6 号试样熔池下流严重,导致试样上部烧穿,下部形成焊瘤.

按图 1a 中 A 处所示位置,分别在 6 个焊接样品的焊缝中部截取试样,每隔 0.5 mm 测一个硬度值,分别在焊缝合金区和热影响区各测得 5 个点取平均值,分别测试了 6 个试样焊缝合金区和热影响区硬度值,测得数据如图 2 所示. 根据测试结果可以看出,1 号,2 号,3 号,4 号试样显微硬度随着焊条中锰含量增加而递增,5 号,6 号试样显微硬度降低,而热影响区没有明显差别. 对 6 个焊接接头进行了抗拉强度测试,接头均在焊缝合金区断裂,测试结果见图 2. 1 号,2 号,3 号,4 号试样抗拉强度随着焊条中锰含量增加而递增,5 号,6 号试样抗拉强度随着焊条中锰含量增加而迅速降低.

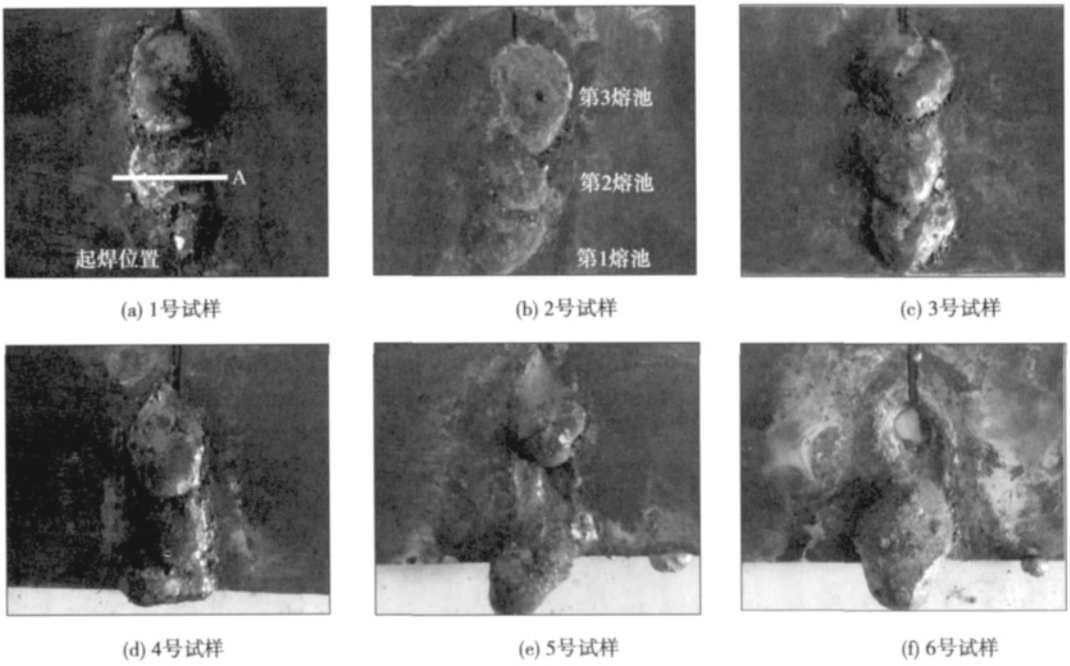

图 1 不同锰含量焊条焊接试样宏观形貌

Fig. 1 Samples by welding rod of different Mn contents

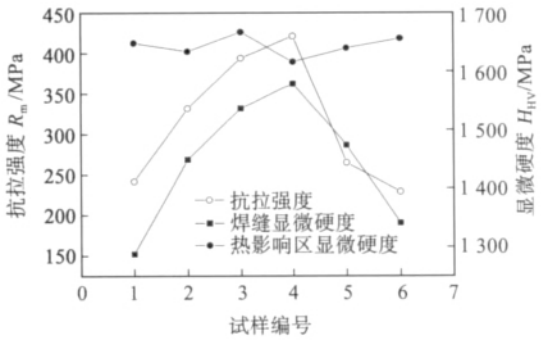

图 2 不同锰含量焊条焊接试样显微硬度与抗拉强度关系曲线

Fig. 2 Micro-hardness and tensile strength of sample by welding rod of different Mn contents

同样按图 1a 中 A 处所示位置,分别在 6 个焊接样品的焊缝中部截取试样并对焊缝合金区进行 SEM 观测并结合 EDS 分析确定焊缝相组成. 图 3 为不同锰含量焊条焊接试样显微组织形貌. 分析得出 1 号试样焊缝中出现大量气孔,富铁相和富铜相区分不明显. 2 号,3 号试样焊缝中气孔显著减少,并且有大量富铁相析出填充焊缝. 随着焊条中锰含量的继续增加,在 4 号试样焊缝中几乎没有气孔,焊缝合金主要为富铁相. 5 号试样富铁相迅速减少,焊缝以富铜相为主,并且有微裂纹出现. 6 号试样焊缝以富铜相为主,裂纹更为明显,并且伴随有少量缩孔出现.

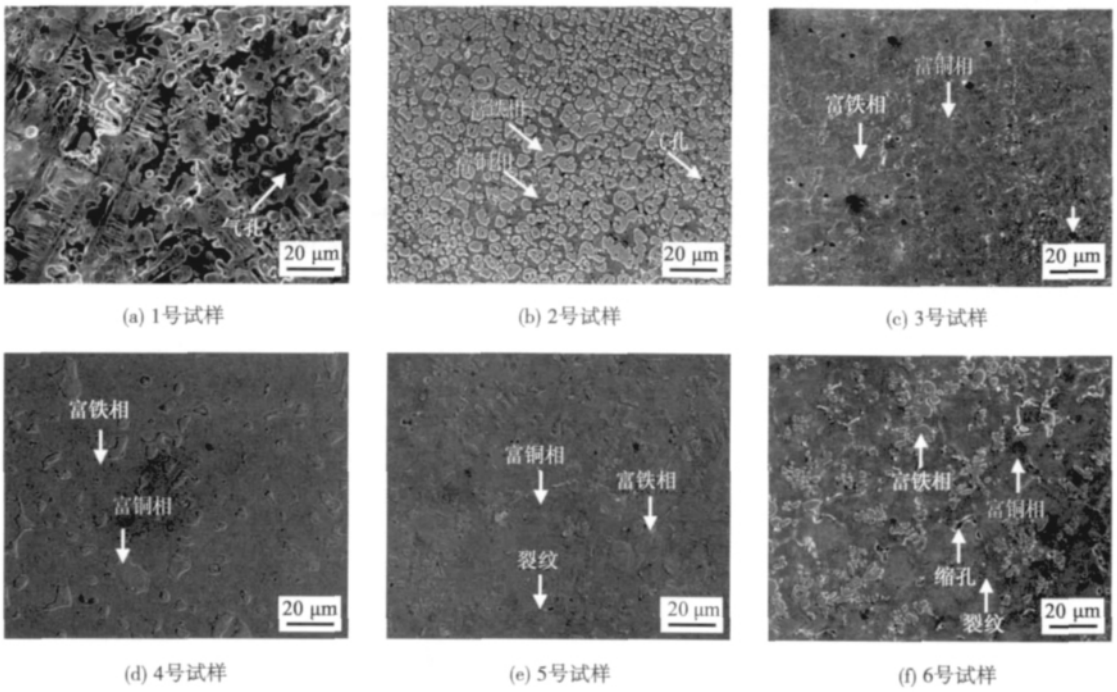

图 3　不同锰含量焊条焊接试样显微组织形貌

Fig. 3　Microstructure morphology of sample by welding rod of different Mn contents

3　分析与讨论

由焊条成分表可知焊接时脉冲燃烧型焊条发生的自蔓延反应主要为

$$3CuO + 2Al = 3Cu + Al_2O_3 + 1\ 519 \quad (1)$$

$$Fe_2O_3 + 2Al = 2Fe + Al_2O_3 + 836 \quad (2)$$

由于高热剂中 CuO，Fe_2O_3 和铝按反应摩尔配比配制，而另外有少量 Fe_2O_3 作为造渣剂添加进焊条中，导致焊条整体反应为铝不足量. 锰为还原剂加入焊条中在高温下可与过剩 Fe_2O_3 反应放出热量. 由图 1 可以看出 1 号焊条完全不添加锰，热量不足，起焊时不能形成有效熔池，影响整体焊缝成形. 随着锰的添加，焊条热量逐渐增大，2 号，3 号，4 号试样焊缝成形良好. 5 号试样由于热量过剩导致熔池开始向下流，在下部形成焊瘤，熔敷金属流失严重. 6 号试样热量过大最终导致下部形成焊瘤，上部母材烧穿.

1 号焊条中没有锰，焊条中过量的 Fe_2O_3 进入熔池参与冶金反应，在高温下发生的反应有

$$2Fe_2O_3 = 4FeO + O_2 \quad (3)$$

$$FeO + C = Fe + CO \quad (4)$$

以上反应产生大量气体，手工自蔓延焊接温度相对其它传统焊接方式温度低，熔池凝固快，熔池金属中的气体在金属凝固前未能及时逸出，从而以气泡的形式残留在凝固的焊缝合金内，导致试样焊缝合金中有大量气孔. 气孔的存在减少了焊缝合金的有效工作断面，显著降低了焊缝合金的强度和塑性; 另一方面因为焊条热量低，焊缝成形差，所以 1 号试样显微硬度和抗拉强度都低. 2 号，3 号焊条中加入锰后，在焊条燃烧过程中发生先期脱氧[7]，即

$$Fe_2O_3 + Mn = 2FeO + MnO \quad (5)$$

$$FeO + Mn = Fe + MnO \quad (6)$$

在 2 号，3 号焊条中锰含量偏低，脱氧反应不完全，最后焊缝凝固成形后有少量气孔，影响接头力学性能. 式(5) 和式(6) 为放热反应，故伴随锰的脱氧反应，焊条放热量增加，有利于焊缝成形. 且由图 3 可看到 2 号，3 号试样焊缝中富铁相占比逐渐增加，富铁相增加有利于接头力学性能提高，故 2 号，3 号试样综合力学性能逐渐升高. 4 号焊条锰含量适当，发生先期脱氧后有 Mn 元素剩余经熔滴过渡进入熔池，发生沉淀脱氧，进一步降低了熔池中的氧势，减少气体的生成，故在焊缝中基本没有气孔. 试验分析 4 号试样发现焊缝合金中仅含微量的 Mn 元素，故可以确定锰不能通过熔滴过渡直接进入合金影响接头性能，与文献[5]研究结果一致. 但锰可以减少焊接缺陷和增加焊缝中富铁相占比，使 4 号试样显微硬度和抗拉强度最高. 5 号焊条中锰含量继续增加，过量的锰被氧化放出热量使得熔池维持在高温的时间加长，使得焊缝中主要析出富铜相，富铜

相显微硬度降低. 另一方面,锰被氧化后增加熔池中熔渣含量,部分熔渣排除不及时,作为熔池杂质富集在晶界,在富铜相凝固后形成液态薄膜,在接头冷却过程中受热应力作用形成裂纹,试样抗拉强度迅速降低. 6 号焊条中锰含量大于 5 号焊条,焊条热量继续增加,熔池温度增高,熔池中杂质增多,在接头冷却过程中热应力相应增大,所以 6 号试样中裂纹宽度显著增加,并有少量缩孔出现,综合力学性能最差.

4 结 论

(1) 脉冲燃烧型焊条立焊时锰不能直接进入焊缝合金,但焊条中锰含量的变化可影响焊缝成形,未添加锰时起焊位置没有形成有效熔池; 锰含量低于 5.9% (质量分数) 时锰含量越高焊缝成形越好; 锰含量超过 5.9% (质量分数) 时,锰含量增加使得熔池向下流动严重形成焊瘤,甚至烧穿母材.

(2) 脉冲燃烧型焊条中锰含量低于 5.9% (质量分数) 时,锰含量越高立焊焊接接头力学性能越高; 锰含量为 5.9% (质量分数) 时接头力学性能最高,抗拉强度可达 421 MPa,显微硬度可达 1 578.8 MPa.

(3) 脉冲燃烧型焊条中未添加锰时,焊缝中有大量气孔; 锰含量低于 5.9% (质量分数) 时随着锰含量增加焊缝中气孔迅速减少,焊缝以富铁相为主且富铁相占比随锰含量增加而增加; 锰含量超过 5.9% (质量分数) 时,焊缝以富铜相为主且有大量裂纹出现.

参考文献:

[1] 李志尊, 辛文彤, 武 斌, 等. 高热剂对低碳钢手工自蔓延焊接的影响 [J]. 焊接学报, 2007, 28(2): 79 - 81.
Li Zhizun, Xin Wentong, Wu Bin, *et al*. Effect of thermit composition on manual SHS welding for low carbon steel [J]. Transactions of the China Welding Institution, 2007, 28(2): 79 - 81.

[2] 辛文彤, 马世宁, 李志尊, 等. Fe 基手工自蔓延焊接接头的组织和性能 [J]. 焊接学报, 2009, 30(10): 73 - 75.
Xin Wentong, Ma Shining, Li Zhizun, *et al*. Structure and property of Fe-base manual SHS welding joint [J]. Transactions of the China Welding Institution, 2009, 30(10): 73 - 75.

[3] 胡军志, 马世宁, 陈学荣, 等. 三种 Cu 基自蔓延焊接材料焊接接头性能的研究 [J]. 材料热处理学报, 2007, 28(3): 81 - 84.
Hu Junzhi, Ma Shining, Chen Xuerong, *et al*. Properties of welding joint prepared using three copper-base SHS welding materials [J]. Transactions of Materials and Heat Treatment, 2007, 28(3): 81 - 84.

[4] 邹家生. 材料连接原理与工艺 [M]. 哈尔滨: 哈尔滨工业大学出版社, 2005.

[5] 桂赤斌, 曾海斌, 吴平安, 等. 气保护药芯焊丝合金元素 C、Mn 过渡行为 [J]. 焊接学报, 2003, 24(2): 86 - 88.
Gui Chibin, Zeng Haibin, Wu ping'an, *et al*. Transfer behaviors of carbon and manganese of flux-cored wire in gas shielded arc welding [J]. Transactions of the China Welding Institution, 2003, 24(2): 86 - 88.

[6] 吴永胜, 王建江, 辛文彤, 等. 脉冲燃烧型立焊焊条 [J]. 焊接学报, 2012, 33(12): 109 - 112.
Wu Yongsheng, Wang Jianjiang, Xin Wentong, *et al*. Pulse combustion welding rod for vertical weld [J]. Transactions of the China Welding Institution, 2012, 33(12): 109 - 112.

[7] 张文钺. 金属熔焊原理及工艺 [M]. 北京: 机械工业出版社, 1980.

作者简介: 吴永胜,男,1985 年出生,博士研究生. 主要从事自蔓延焊接技术研究与应用工作. 发表论文 8 篇. Email: wuysh. 2007@163. com

通讯作者: 王建江,男,教授. Email: JJWang63@ heinfo. net

China; 2. Capital Aerospace Machinery Company, Beijing 100076, China). pp 93 – 96

Abstract: Limit loads of strength mismatched welded joints with asymmetric cracks were calculated using finite element method, and the effect of crack location on the limit load of strength mismatched welded joint was investigated. The results show that when the weld slenderness (the ratio of crack ligament to the half-weld width) was small, the limit load of welded joint was close to that of homogeneous welded metal plate with the same geometry. With the increase of slenderness, the limit load of welded joints with different strength mismatched factors converged and the influence of strength mismatching decreased. For a given strength mismatched factor, crack eccentricity had great influence on the limit load of welded joint when the weld slenderness was small, the limit load of under-matched joint increased with the increase of crack eccentricity, while for over-matched joint, the opposite was true. With the increase of weld slenderness, the effect of crack eccentricity on the limit load decreased.

Key words: strength mismatch; asymmetric crack; limit analysis; limit load; finite element method

Influence of Mn on microstructure and properties of vertically welded joint with pulse combustion welding rod

WU Yongsheng[1], WANG Jianjiang[1], XIN Wentong[1], QU Lifeng[2] (1. The Institute of Advanced Materials, Ordnance Engineering College, Shijiazhuang 050003, China; 2. Military Delegate Office of Chongqing Martial Delegate Agency in No. 167 Factory, Chengdu 610110, China). pp 97 – 100

Abstract: Q235 steel was welded by manual high-temperature synthesis (SHS) vertical welding process with pulse combustion welding rod, and the influence of Mn content on the microstructure and properties of the resultant joints were studied. The results show that, without adding Mn in the pulse combustion welding rod, massive pores appeared in the weld without forming effective weld pool at the starting position of welding. When the Mn content was less than 5.9 wt%, the higher the Mn content was, the better the weld was shaped, and the pores reduced rapidly. Fe-rich phases dominated in the weld with the proportion increasing with the increase of Mn content, and the mechanical properties of the joints also increased. When the Mn content was 5.9wt%, the mechanical properties of the joints reached the optimum with tensile strength of 421 MPa and microhardness of 1 578.8 MPa. When the Mn content exceeded 5.9wt%, the increase of Mn content resulted in the weld pool flowing downward seriously and forming welding beading or even burning through the substrate. The resulting weld mainly comprised Cu-rich phases with lots of cracks, which deteriorated the mechanical properties of the joint.

Key words: plus combustion welding rod; vertical welding; microstructure

Narrow gap pulsed MAG welding of 40CrMnMo thick-walled pipe

BA Lujun[1], MA Caixia[2], ZHANG Tiejun[1], WANG Jun[1], WANG Qinglin[1] (1. Drilling Pipe and Tools Company, Shengli Petroleum Administration Bureau Bohai General Drilling Compang, Dongying 257200, China; 2. Shaanxi Key Laboratory of Friction Welding Technologies, Northwestern Polytechnical University, Xi'an 710072, China). pp 101 – 104

Abstract: Considering the structure characteristics of small-diameter thick-walled pipe and the properties of 40CrMnMo steel, narrow gap pulsed MAG welding technique was preferred to weld the oil drill collars. A large number of experiments were conducted to improve the gas protection, arc morphology and stability, and weld appearance to avoid the sidewall fusion defects during welding, and the narrow gap multi-layer welding parameters were optimized. Furthermore, a new special narrow gap welding torch was designed, which had advantages such as simple and compact structure, good accessibility, good gas protection, easy ignition, stable arc combustion and free from sidewall ignition. The mechanical tests and microstructure analysis show that the mechanical properties of joints can satisfy the practical requirements of the oil drill collars.

Key words: oil drill collars; narrow gap pulsed MAG welding; weld appearance; joint property

Numerical simulation of resistance spot welding of three-layer galvanized steel sheets

LU Changjin[1], TANG Hong[1], YAO Qiwei[2], YU Miao[2], SHEN Qing[2], LEI Ming[3] (1. Shanghai Key Laboratory of Laser Manufacturing & Material Modification, Shanghai Jiaotong University, Shanghai 200240, China; 2. SGM Dongyue, Dongyue 264006, China; 3. Baoshan Iron and Steel Co., Ltd., Shanghai 201900, China). pp 105 – 108

Abstract: Based on the characteristics of resistance spot welding of three-layer sheets and properties of zinc coating, 1/4 model was established to numerically simulate the three-layer sheets. On the basis of experimental parameters, the nugget was investigated through optimizing the parameters. Then under the peak temperature, nugget formation and growth in different materials were analyzed with the optimized parameters. It was found that, comparing to the sheets without Zn coating, the Zn coating can affect the nugget formation, change the location of nugget nucleation and growing trend. For three-layer galvanized sheets, the nugget initially formed in the interface between two sheets without Zn coatings, and then grew radially and axially, finally penetrated three sheets. The simulated results agreed well with the experimental results.

Key words: spot welding; three layer board; numerical simulation; zinc coating; nugget

Analysis of buckling distortion caused by welding using 3D optical measurement technology

SUN Xiangwei[1], YIN Xianqing[1], WANG Jiangchao[2], ZHANG Jianxun[1] (1. State Key Laboratory for Mechanical Behavior of Materials, Xi'an Jiaotong University, Xi'an 710049, China; 2. Joining and Welding Research Institute, Osaka University, Osaka 5670047, Japan). pp 109 – 112

Abstract: 3D optical surface scanning method was used in this paper to investigate the buckling distortion of mild-steel plate during bead-on welding. The full field distortions were obtained through measuring the deformation of the plate before and after welding, respectively. Based on the numerical simulation on the elastic buckling distortion with inherent strain method, it was found that the concave-convex type distortion belonged to buckling distortion. The residual stresses were measured with hole-drilling method, and the results showed that the high longitudinal compressive stress existed in the zone away from the weld, which resulted in the buckling distortion of the plate. Combining with numerical simulation, the 3D optical surface scanning system could be used to accurately investigate the buckling mechanism of welded thin plate.

Key words: 3D optical surface scanning; thin plate; GTAW; buckling distortion; inherent strain method